Quantum Electronics **50** (7) 614–622 (2020) ©2020 Kvantovaya Elektronika and IOP Publishing Limited

https://doi.org/10.1070/QEL17288

Holographic wavefront sensors

V.Yu. Venediktov, A.V. Gorelaya, G.K. Krasin, S.B. Odinokov, A.A. Sevryugin, E.V. Shalymov

Abstract. **A brief historical review of the first designs of holographic wavefront sensors (WFS's) and the concepts lying in their basis is presented. The main directions in the development of these sensors are highlighted and considered. One of these directions implies a two-stage transition from the use of several separate measuring channels with holograms filtering only one Zernike mode: first to the use of one channel with a multiplexed hologram filtering several first Zernike modes, and then to filtering the entire set of Zernike modes with the aid of one combined multiplexed hologram. Another line of research in this field (related to the first one) is the optimisation of the filter hologram structure in order to reduce cross-modulation interferences, increase multiplexing level, etc. One more line of research implements principles of dynamic holography by introducing spatial light modulators into the WFS composition. Hence, the advantages of time multiplexing of holograms can be used. The approach developed by G. Andersen's team, aimed at adapting the holographic WFS design for operation as an element of adaptive optical system with a zonal corrector, as well as an approach implying development of hybrid holographic sensors, are considered separately. The results of the authors' studies of holographic WFS's with application of the methods of Fourier holography (i.e., holography of focused beams, in particular, using diffuse scatterers in a hologram recording channel) are also reported.**

Keywords: *adaptive optics, Zernike polynomials, expansion in the basis, holographic filtering, holographic wavefront sensors.*

1. Introduction

Wavefront sensors (WFS's) are devices for measuring deviations of a light wavefront from a plane or sphere. Currently, optical WFS's are widely used to design adaptive optical systems in various fields of science and technology: astronomy, microscopy, laser technique, ophthalmology, and many others [1–5]. The wavefront shape is directly related to the spatial distribution of the wave phase. However, as is known, the current technological level does not make it possible to perform direct measurements of the light wave phase. In this context, the operation of all WFS's is based on the transformation of a wave phase distribution into an intensity distribution, recorded by photodetectors, and subsequent recalculation of photodetector signals into wave phase distortions (calculation of local phase distortions or wave aberrations). There are several classical types of sensors in which the transformation of a phase distribution into an intensity distribution recorded by photodetectors is based on the principles of optical interferometry or geometric optics [6–10].

Shear interferometers are generally used in interferometric WFS's. The input wavefront is split into two or more waves, one of which plays the role of a reference wave. Then the waves are converged and interfere. The thus obtained interference pattern (or patterns) is (are) determined by the initial-wavefront phase distribution. However, the range of application of interferometric WFS's is rather limited, because they are sensitive to vibrations and allow one to measure only small wavefront distortions; at the same time, the processing of their interference patterns is rather complicated and calls for a longer time than in the case of other sensors.

More popular WFS's are those based on the analysis of the intensity distribution in some image or a set of images. These devices include Shack–Hartmann WFS's, curvature sensors, pyramidal sensors, etc. To date, Shack–Hartmann WFS's are most popular ones. In these sensors, narrow beams are cut [using a lens array (a matrix of identical microlenses)] from a wavefront under study and focused on a photodetector (for example, a CCD array). The images formed by the lenses are displaced because of the wavefront distortion. The displacement value and direction for the image formed by an individual lens are determined by the local wavefront inclination on the lens aperture. Then, the wavefront shape is reconstructed from local parameters using rather cumbersome calculations. This circumstance limits significantly the operating speed of systems of these types. In some cases (primarily for atmospheric optics problems), WFS's with a data renewal rate of 1–10 kHz or even higher must be applied. Using optimised processing algorithms and highly efficient computers for Shack–Hartmann sensors, one can develop optical adaptive systems operating with a frequency of a few kHz. However, such systems are fairly complicated and expensive. Indeed, to provide an acquisition frequency of 1 kHz for the wavefront-shape data, one must provide a processing rate of several Gb s^{-1}. The same holds true for the other WFS's mentioned above.

It is of prime importance that all these sensors, including interferometric ones, are *zonal*. In other words, the arriving wavefront is divided into segments (zones). Then the system calculates a particular wavefront parameter (tilt, curvature,

V.Yu. Venediktov St. Petersburg Electrotechnical University LETI, ul. Prof. Popova 5, 197022 St. Petersburg, Russia; Faculty of Physics, St. Petersburg State University, Universitetskaya nab. 7/9, 199034 St. Petersburg, Russia; e-mail: vlad.venediktov@mail.ru;
A.V. Gorelaya, A.A. Sevryugin, E.V. Shalymov St. Petersburg Electrotechnical University LETI, ul. Prof. Popova 5, 197022 St. Petersburg, Russia;
G.K. Krasin, S.B. Odinokov Bauman Moscow State Technical University (National Research University), Vtoraya Baumanskaya ul. 5, 105005 Moscow, Russia

Received 18 February 2020; revision received 3 April 2020
Kvantovaya Elektronika **50** (7) 614–622 (2020)
Translated by Yu.P. Sin'kov

etc.) within each zone, after which the wavefront shape is reconstructed by matching the data for all zones. Generally, a user obtains final information about the wavefront in the form of its expansion in Zernike polynomials (modes) or in some other basis; in most cases, one needs data on a relatively small number (up to 20–30) of these modes. Thus, the use of all zonal sensors is related to a large amount of calculations that are necessary to acquire data on several output parameters. Therefore, the development of modal sensors, in which these parameters are measured directly, should simplify significantly the design of WFS's and reduce their cost, with a simultaneous significant increase in their operating speed. Specifically these approaches are considered below.

Holographic sensors hold a particular position among zonal WFS's. The transformation of phase distribution into intensity distribution in these sensors is performed due to the holographic filtering of local wavefront aberrations or aberration modes. To date, holographic WFS's are needed to design adaptive optical systems in which Shack–Hartmann sensors and similar WFS's cannot be used; i.e., when the desired renewal rate exceeds several kHz and/or application of large-size and expensive computers is excluded. Holographic sensors can operate with a high frequency, because, when using simple algorithms to process photodetector signals, they yield information about the wavefront in the form of only several dozens of numbers: amplitudes of aberration modes (for example, Zernike modes) or adaptive-mirror modes. Thus, the signal from these sensors can be applied, practically without any additional processing, to control directly the shape of adaptive mirrors. Holographic WFS's have a high potential in such fields as confocal and two-photon microscopy [11], light source positioning [12, 13], optical communication in free space [14], ophthalmology [15], adaptive optics [16], and direct ultrafast recording by laser beams [17]. They are especially urgent in problems where amplitudes of only several first Zernike modes must be estimated. The range of application of holographic sensors is expected to expand in the future due to their simplicity, wide dynamic range, and high potential sensitivity.

2. First publications devoted to zonal and holographic WFSs

The study by M.A.A. Neil et al. [18] became the first publication devoted to holographic WFS's. A new principle of designing modal WFS's was theoretically considered in it. Initially, before holograms came into practice, these sensors provided measurement of only a limited number of aberration modes of the wavefront arriving at them [19–22]. For example, under certain conditions (the wavefront intensity fluctuations are negligible, higher order aberration modes are absent or negligible, etc.), a meter of light intensity momenta makes it possible to estimate indirectly four lower aberration Zernike modes [21]. The principle of constructing modal WFS's that was proposed in [18] allows one to measure directly the value of any chosen aberration Zernike mode existing in the wavefront studied. Initially, the authors considered their concept by an example of modal sensor based on a phase plate (Fig. 1) and then proposed a modified version, in which the input wavefront was subjected to holographic filtering (Fig. 2).

The principle of constructing modal WFS's that was proposed in [18] is clarified in Fig. 1. The input wavefront is divided by a beam splitter into two identical waves, which are

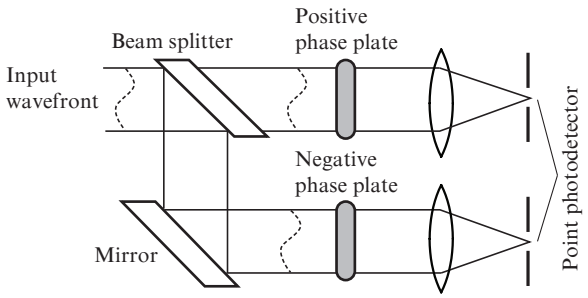

Figure 1. Principle of building up a modal WFS proposed by M.A.A. Neil and co-workers.

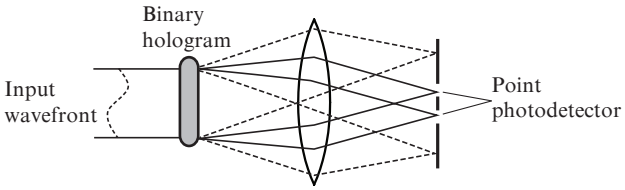

Figure 2. WFS based on a binary hologram.

transmitted through two phase plates; one of these plates is positive and the other is negative. The positive phase plate distorts the wave, increasing one of the aberration Zernike modes by some value. The negative phase plate decreases the same aberration Zernike mode (subtracts this aberration). To implement optical Fourier transform, the phase plates are located in the rear focal plane of the lenses. Then both waves are focused on point photodetectors. In the first approximation, the difference in the intensities of these two waves is proportional to the amplitude of the aberration Zernike mode existing in the initial wavefront. Thus, one can construct a modal holographic WFS using two optical channels with phase plates for filtering each of the aberration modes. However, this approach is impractical, because the number of measuring channels increases proportionally with an increase in the number of measured aberration modes, and the sensor design becomes cumbersome.

In this context, Neil and coworkers proposed an alternative approach, based on the use of holographic filtering (Fig. 2). Here, instead of beam splitters with phase plates, one uses a previously computed binary diffraction element (phase binary hologram, i.e., a hologram, each structural element of which corresponds to one of two phase levels differing by π rad), combining the holograms of several aberration Zernike modes of interest (i.e., the measured ones). When a beam passes through this binary hologram, the aberration modes coinciding with those recorded in the hologram are filtered off in specified directions and arrive at photodetectors with a small entrance aperture (Fig. 2). Thus, Neil et al. [18] were the first to put forward and consider the concept of developing a holographic WFS. They proposed to use either several individual diffraction elements (holograms), each to filter one of Zernike modes, or one time- or space-multiplexed element (multiplexed hologram) for holographic filtering. In addition, it was shown in [18] that the sensor under consideration has the following feature: when measuring any chosen aberration Zernike mode, there arises a measurement error due to the presence of other aberration Zernike modes in the initial wavefront (intermodal interference). In other words, there is

some spurious sensitivity of the system to other aberration modes. Having optimised the size of photodetector apertures and the value of phase distortions introduced by the hologram (the amplitude of the aberration mode recorded in the hologram), one can reduce the spurious sensitivity.

Later on, the authors of [18] were the first to demonstrate in practice the operation of holographic WFS's [11, 23]. They implemented an adaptive system with a closed feedback loop, consisting of a wavefront generator, an aberrating medium, and a modal holographic WFS; a schematic diagram of this system is presented in Fig. 3. Due to the use of a ferroelectric liquid-crystal spatial light modulator FLCSLM1, a wavefront of specified shape was generated. This device served as a master element. Then the wave passed through the aberrating medium (a piece of poor-quality glass). To filter off aberration modes, the WFS was equipped with a static binary hologram, implemented on the second ferroelectric liquid-crystal spatial light modulator FLCSLM2. A CCD camera installed in the lens focal plane fixed diffraction spots corresponding to 16 aberration Zernike modes and the spot corresponding to zero diffraction order.

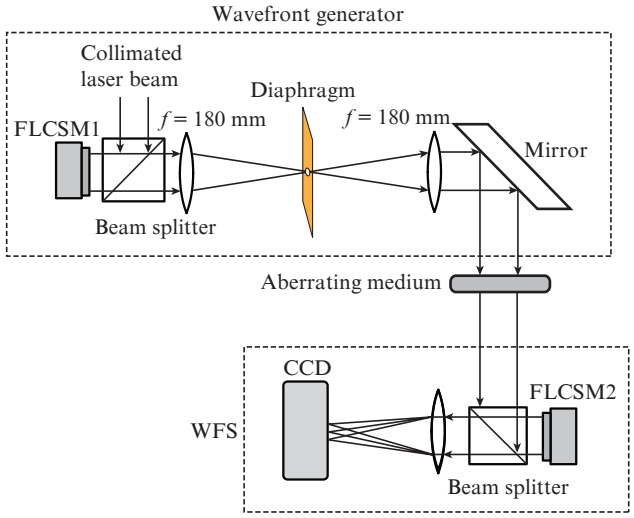

Figure 3. Adaptive system with holographic WFS and closed feedback loop.

The operating speed of the adaptive system in the experiment was significantly limited by the operating speed of the CCD camera and the imperfection of the signal-processing software. As a result, the adaptive system performed only about three iterations per second. The operation of the system was estimated by measuring the Strehl number of the spot corresponding to zero diffraction order. The Strehl number increased from 0.4 to 0.9 or more after five iterations and approached 1.0 after ten iterations.

3. Application of multiplexed holograms for filtering aberration modes and optimising their structure

The use of several individual channels with holograms filtering only one of aberration modes in modal WFS's is unpractical, because in this case the sensor becomes cumbersome, and the intensity of the radiation incident on each of the holographic elements decreases (inversely proportionally to the squared number of channels). In this context, the tendency of researchers to use spatially superimposed (multipole) holograms for filtering looks justified [24–27]. The most widespread orthogonal basis for expanding wavefront aberrations in series is Zernike polynomials. For some specific applications it is more convenient to perform expansion in functions of other types, for example, Fourier or Karhunen–Loeve functions [13, 28, 29].

Despite the advantages of multiplexed holograms, their use for filtering aberration modes leads to the occurrence of cross-modulation interferences. To measure N aberration modes, one must apply a multiplexed hologram composed of at least N subholograms [26, 30]. Thus, with an increase in the number of measured aberration modes, the number of subholograms increases proportionally, and, as a consequence, the cross-modulation interferences increase as well. To reduce the magnitude of cross-modulation interferences, one should optimise the filter hologram design, the amplitude of aberration modes recorded in the hologram, the aperture sizes, the positions of photodetectors, and the number of recorded aberration modes. However, since these parameters affect also the magnitude of intermodal interferences, the measurement range, and the sensitivity, the optimisation problem becomes fairly difficult [25, 26]. It should be noted that, when multiplexed holograms are used for wavefront filtering in practice, there arise errors caused by the nonideality of not only the hologram reconstruction but also the hologram recording. In addition, when recording superimposed holograms, it is generally practically impossible to provide optimal values of diffraction efficiency, which leads to inexpedient energy losses in the analysed beam. The recording-induced errors may prevail when recording holograms of aberration modes (especially of higher orders) on a photosensitive film. However, applying computer (digital) synthesis and multiplexing of filter holograms, one can reduce these errors to minimum (to a negligible level). In addition, the use of the principles of digital holography provides a large freedom in optimising filter holograms and simplifies them [31].

The range of carrier frequencies that can be used to code a WFS multiplexed hologram is limited from below by the geometric size of the recording medium (a photodetector film diameter or a spatial phase modulator length) and from above by the minimum size of a hologram resolution element (pixel size for a photodetector or a spatial phase modulator). In addition, carrier frequencies can be chosen only from some series of fixed values, for which an integer number of resolution elements corresponds to the carrier frequency half-period (in order to exclude ?moiré effects); when the carrier wave vectors are oriented identically, their magnitudes should not be multiple of each other. There are different approaches to the orientation of carrier wave vectors. They can be classified with respect to the arrangement of the diffraction spots formed by the carrier waves: circular type (Fig. 4a), columnar type (Fig. 4b), square type (Fig. 4c), quadrant type (Fig. 4d), and axial type (Fig. 4e) [32]. It should be noted that filter holograms can be recorded using different spatial multiplexing methods: superimposition of subholograms (recording them in the same photodetector area one over other) [33] or composing subholograms (or their individual portions) into a matrix filling the filter hologram aperture (subhologram portions alternate in a checkerboard order, in the form of concentric rings, etc.) [32, 34]. The choice of the magnitudes and directions of carrier wave vectors is determined by an increase

in the level of noise and intermodal interferences, which is observed when the diffraction spots corresponding to aberration modes approach each other and the central maximum (first diffraction order). In addition, the choice of the approach to the orientation of carrier wave vectors, in combination with the spatial multiplexing type, affects the diffraction efficiency of hologram and the sensitivity of a sensor on its basis [32]. The diffraction efficiency of hologram can be increased additionally by its binarisation [30, 33].

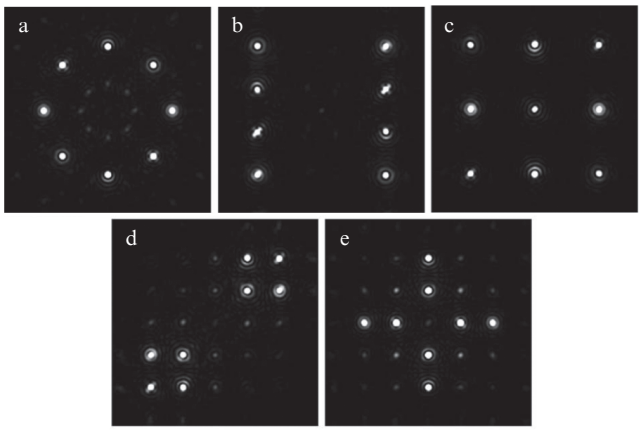

Figure 4. Distributions of diffraction spots for (a) circular, (b) columnar, (c) square, (d) quadrant, and (e) axial types of orientation of carrier wave vectors.

When recording or synthesising holograms in a modal sensor, both plane [29, 33] and spherical waves [34, 35] can be used as reference ones. With spherical waves, the sensor design can be simplified. In this case, each reference wave converges in a photodetector region specially assigned for it (Fig. 5). As a result, when carrying out reconstruction, one does not need any additional lens to perform optical Fourier transform.

As was noted in the previous section, the difference in the intensities of two symmetric diffraction spots, corresponding to the positive and negative amplitude values for some aberration mode, is proportional to the amplitude of this mode only in the first approximation. The output characteristic of a modal holographic sensor is close to linear only within a limited range. This range is somewhat narrower (to what extent, it depends on the hologram design) than the difference between the positive and negative amplitudes of the aberration modes recorded in a filter hologram. Nevertheless, an increase in the amplitudes of the aberrations recorded in the hologram not only expands the measurement range but also reduces the slope of the output characteristic, and, therefore, deteriorates sensitivity. In addition, if the amplitudes of recorded aberrations exceed some value (determined by the hologram parameters), the linearity of the output characteristic decreases. Therefore, the measurement range of developed modal holographic sensors does not generally exceed several wavelengths [31, 33]. The measurement range of a holographic sensor can be expanded without loss of sensitivity if each of the aberration modes is detected using a set of M subholograms with different aberration amplitudes (differing, for example, by half wavelength) [36]. However, this approach is inefficient, because the number of multiplexed holograms increases by a factor of M; correspondingly, cross-modulation interferences increase as well [31].

When optimising a holographic sensor, one should pay attention to the size (diameter) and position of the photodetector sensitive areas. The optimal size of photodetector apertures, at which the level of WFS interference and noise is minimal, corresponds to each fixed amplitude of the aberration modes recorded in the hologram. In addition, the sensor sensitivity decreases with increasing the aperture size [26, 35]. Both photodiodes and CCD or CMOS matrices can be applied as photodetectors. When using photodiodes, the recording rate can be increased. However, the centroids of the diffraction spots corresponding to aberration modes may shift during WFS operation, for example, because of misalignments. In the case of photodiodes, this effect leads to instability of output characteristic. When a CCD- or CMOS matrix is used, the sensitivity to the shift of diffraction-spot centroids can be reduced due to the dynamic displacement of photodetector aperture (choice of pixels) and application of special algorithms for calculating the diffraction-spot intensity [26, 37].

4. Application of dynamic holography principles in WFS's

The problem of cross-modulation interferences can be solved by passing to temporal multiplexing of holograms. In this case, holograms filtering only one Zernike mode or several such modes are successively formed on the same optical ele-

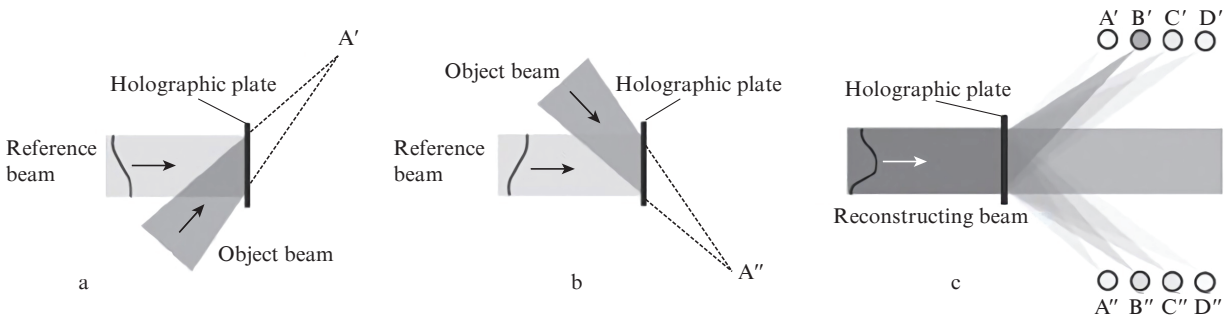

Figure 5. Use of spherical waves as reference ones when forming a multiplexed hologram WFS: (a) recording of the interference pattern (subhologram) of a spherical wave converging at a point A′ and an aberration mode with a positive amplitude, (b) recording of the interference pattern (subhologram) of a spherical wave converging at a point A″ and the same aberration mode with a negative amplitude, and (c) reconstruction of a multiplexed hologram consisting of four pairs of subholograms.

ment [14, 18, 38]. Dynamic holograms can be implemented using liquid-crystal spatial phase modulators, for example LETO (resolution 1920× 1080, pixel step 6.4 μm, input frame rate up to 180 Hz) or GAEA-2 (resolution 4160× 2464, pixel step 3.7 μm, input frame rate 59 Hz), manufactured by HOLOEYE. It was experimentally demonstrated that holographic WFS's with temporal multiplexing can successfully be applied in wireless optical communication lines to measure phase aberrations during their correction [14]. F. Feng and colleagues designed a sensor based on nematic liquid-crystal phase spatial light modulator (resolution 1280×768, pixel size 13 μm), to which holograms corresponding to Zernike polynomials from astigmatism to quatrefoil were successively applied. An adaptive system equipped with that WFS made it possible to measure and correct intrinsic aberrations of the system and random phase aberrations (to 0.15 wavelength λ per probe–correction cycle) caused by atmospheric turbulence. When implementing a closed-loop algorithm for correction, aberrations of larger size (more than 0.15λ) can be found and corrected for several correction cycles [14].

A negative effect of temporal multiplexing is the decrease in the operating speed of holographic WFS's, which is proportional to the number of measured Zernike modes. Nevertheless, this approach is justified when cross-modulation interferences must be maximally suppressed or when only few aberration modes should be determined (for example, in ophthalmology). Temporal multiplexing can also be used jointly with spatial. In other words, several multiplexed holograms are successively formed on a spatial phase modulator, and each of them filters off only few aberration modes [38]. This approach would provide a compromise between the sensor operating speed and the level of cross-modulation interferences. It should be noted that the technical characteristics (pixel size, switching time, etc.) of modern spatial phase modulators do not make it possible to implement high-quality fast holographic WFS's on their basis. However, in view of the continuous development of liquid-crystal light modulators, the use of temporal multiplexing may become justified in the nearest decade.

Using the principles of dynamic holography, one can also probe and correct the light wavefront using the same spatial phase modulator [14, 39]. These operations can be performed either successively [14] or simultaneously [39]. In the former case, the above-described mechanism of temporal multiplexing is involved. In the latter case, a complex hologram consisting of several subholograms is formed on phase spatial modulator; this hologram simultaneously filters off aberration modes and corrects distorted wavefront (Fig. 6).

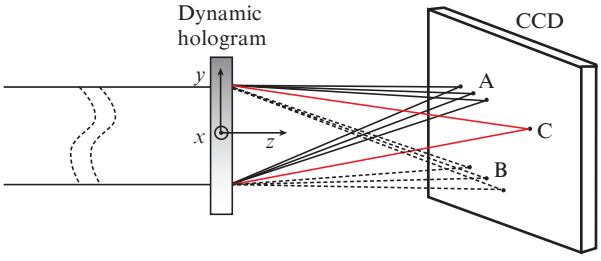

Figure 6. Principle of operation of dynamic holographic adaptive system.

To filter off n aberration Zernike modes, n pairs of subholograms should be used. One subhologram from a pair corresponds to the interference pattern formed by some ith Zernike mode $bZ_i(x,y)$ and a reference spherical wave converging at some point A. The second subhologram corresponds to the interference pattern formed by the same mode Zernike but with negative amplitude $(-bZ_i(x,y))$ and a reference spherical wave converging at some point B. To correct initial-wavefront distortions and construct an image at point C, one should use another subhologram with a complex amplitude transmittance in the form

$$H(x,y) = \Lambda \exp\{-jk[(x - x_C)^2 + (y - y_C)^2 + z_C^2]^{1/2}\},$$

where Λ is a scale factor, which can be used to change the ratio of the fraction of image energy (at point C) to the total energy in the diffraction spots of the subholograms filtering aberration modes.

A schematic of the dynamic holographic adaptive system, whose operation principle was implemented experimentally, is shown in Fig. 7 [39]. The light source was a helium--neon laser with $\lambda = 632.8$ nm. The liquid-crystal spatial light modulator LC-SLM, applied for probing and correcting the wavefront, had a resolution of 256×256 pixels with a pixel size of 24 μm; the diffraction efficiency was 71.5%. Eight Zernike modes were filtered off in the experiment: Z(2,0), Z(2,–2), Z(2,2), Z(3,–1), Z(3,1), Z(3,3), Z(3,–3), and Z(4,0). Thus, 17 imposed subholograms were formed on the light modulator LC-SLM. The Zernike mode amplitudes in subholograms were ±0.251, and the factor Λ was 1/23. A CCD camera with a resolution of 1920×1080 pixels and a pixel size of 7.4 μm served a photodetector. When switching on the system, it was necessary to perform seven correction cycles to control introduced aberrations.

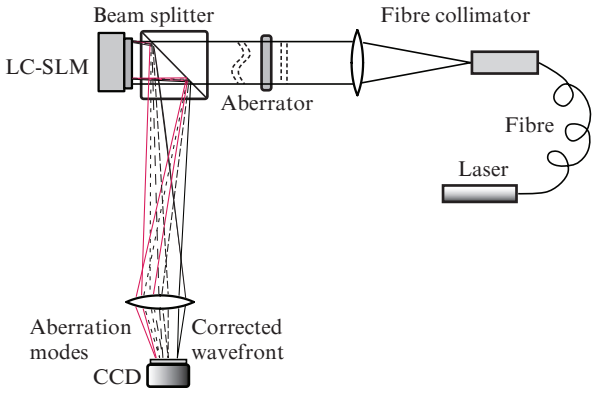

Figure 7. Schematic of an experimental setup implementing dynamic holographic adaptive system.

Based on these results, a method allowing one to measure aberrations of laser beam wavefront using a computer-synthesised Fourier hologram and a spatial phase light modulator was developed and experimentally verified. In this method, the wavefront measurement is divided into two stages. In the first stage, the range in which the desired aberration value falls is roughly estimated (one determines the amplitudes of the aberration modes recorded in the filter hologram that are optimal for the measured wavefront). In the second stage, the

aberration is exactly estimated based on the methods of local optimisation of the objective function. This approach makes it possible to extend the range of measurements preserving at the same time their high sensitivity [40–42]. In the future (in view of the development of spatial phase modulators), holographic WFS's based on the above-described method may compete with interferometric and Shack–Hartmann sensors in problems where a bandwidth of 60–120 Hz is sufficient but exact measurements must be performed in a wide range of phase fluctuations and on apertures exceeding 10 mm. These advantages of holographic sensor also make it possible to apply it in the modal regime without preparing high-precision references.

5. Application of diffuse Fourier holography

A promising way to design WFS's is based on the use of diffuse Fourier holography [43], which in theory should help to exclude cross-correlation interferences. These interferences are the response of photosensitive matrix caused by incorrect energy transfer by multiplexer components; the structure of this response is similar to the measured distortion but is not related to it. The use of a scatterer leads to the occurrence of noise characteristic of holograms with an extended reference source, which are also referred to as holograms with a coded reference beam. The noise intensity for these holograms is equal to the signal intensity (here, the signal is the correlation peak, and the noise is the wide plateau of the autocorrelation function). If the number of holograms recorded with an extended reference source is equal to $2N$, the ratio of the signal intensity from any superimposed hologram in the plane of photographic plate to the intensity of noise formed by the entire holographic plate does not exceed $1/(2N)$. It should be noted that the intensity of the characteristic noise induced by the scatterer can easily be reduced applying spatial filtering.

In this case, the sensor contains a hologram consisting of individual portions; two superimposed Fourier holograms, detecting one of the Zernike modes, are recorded in each portion. While recording, a wave containing one of Zernike modes with a positive amplitude and an object wave, incident on the surface of recording medium at some angle, are directed to the portion of a recording medium through a scatterer and a focusing system performing a Fourier transform. A mobile diaphragm, mounted in front of the holographic plate, makes it possible to choose a region on it to record one of matrix holograms. Then the angle of incidence of the object wave varies, the sign of the Zernike mode amplitude changes to opposite, and the second hologram is recorded on the same portion. Other portions of the hologram are recorded in the same way after displacing the diaphragm. A schematic diagram of recording is presented in Fig. 8.

A proposed schematic of a sensor based on diffuse Fourier holography is shown in Fig. 9. When carrying out a measurement, the wavefront is transmitted through a scatterer and a focusing system (similar to those used in recording) and passes through a matrix of holograms. Along with scatterer S, lens L1, and hologram matrix HM, the sensor contains two microlens arrays MLAs, with the aid of which reconstructed object waves are focused on photodetectors PD, and a set of diaphragms D2, which filter off the scatterer-introduced noise from the radiation incident on the photodetectors. To date, first experimental data have been obtained with this sensor [44]. Further on, its efficiency is planned to be verified in more detail.

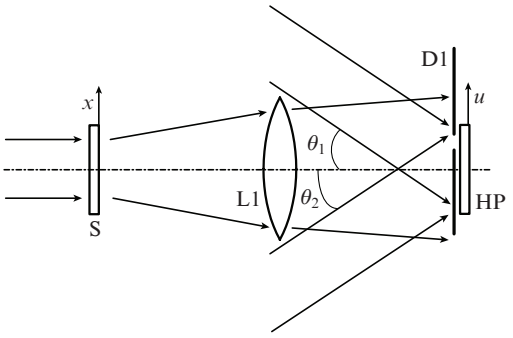

Figure 8. Schematic diagram of hologram matrix recording: (S) scatterer mounted in the front focal plane of lens L1; (D1) mobile diaphragm; (HP) holographic plate.

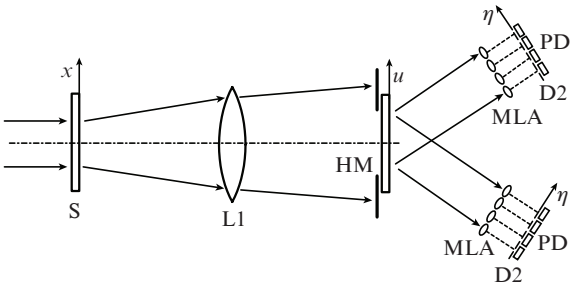

Figure 9. Schematic of wavefront sensor: (S) scatterer; (L1) lens; (HM) hologram matrix; (MLA) microlens array; (D2) diaphragm installed in the focal plane of microlenses; (PD) photodetectors.

6. Zonal holographic WFS's

Based on holographic filtering, one can implement not only modal but also zonal WFS's. The principle of operation of this sensor, proposed by G. Andersen [45] (United States Air Force Academy, United States), is a kind of compromise between the above-described holographic WFS and conventional zonal approach. It is based on the same concept as the modal sensor; however, instead of measuring aberration modes, the depth of local distortions in each wavefront 'zone' is measured in this case. Here, the term 'zone' indicates wavefront partition into individual subapertures, as in conventional Shack–Hartmann or curvature sensors. The operation principle of a zonal holographic WFS is illustrated in Fig. 10.

Thus, Andersen developed a concept of holographic WFS and adapted it for operation as a component of optical adaptive system with a zonal corrector. In this case, one uses a segmented (mosaic) hologram divided into square zones, and only two superimposed subholograms (similar to those considered in Fig. 10) are recorded in each zone. They are recorded by convergent spherical waves and the waves corresponding to the maximum and minimum accumulated phase differences (piston shift) that are expected in a given beam zone. The entire mosaic hologram can be recorded in only one substrate. Certainly, this device provides information not about minimally required 2–30 amplitudes but about approximately several hundreds of local wavefront distortions. Nevertheless, even in this case the gain in the operating speed and computational resources is obvious. Though, it should be noted that zonal correctors (i.e., segmented mirrors) are generally much more complicated and

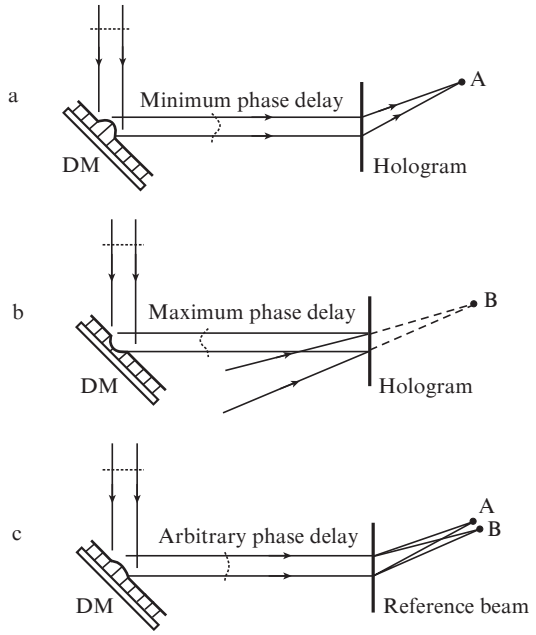

Figure 10. (a, b) Recording of a multiplexed hologram corresponding to the distortion of wavefront in a certain zone with maximum (a) positive and (b) negative amplitudes and (c) its reproduction; DM is a deformed mirror.

expensive than the modal correctors of bimorph-mirror type and other similar devices.

The above-described approach was used to implement a real prototype of inexpensive and fast adaptive optical system with a closed feedback loop, which does not involve any complicated computations (Fig. 11) [46]. When a distorted wavefront arrives at the adaptive system, the difference in the intensities of pairs of symmetric spots is proportional to the signal that must be supplied to the corresponding drives of zonal corrector to eliminate wavefront aberrations.

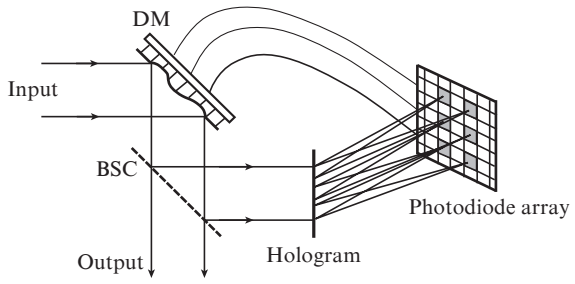

Figure 11. Simple fast adaptive system that does not require any complex computations [46]; BSC and DM stand for beam-splitting cube and deformed mirror, respectively.

It should be noted that one can minimise cross-modulation interferences using this holographic sensor, because in this case each portion of filter hologram consists of only two superimposed holograms. Obviously, this scheme is fairly convenient when adaptive mirrors with 'zonal' control are applied: it is sufficient to match the sizes of mirror zones and mosaic hologram. These segmented mirrors are available; however, they are much more expensive than continuous flexible mirrors with 'modal' control, for example, well-known bimorph mirrors. Therefore, despite the successful demonstration of a zonal holographic WFS, the problem of designing a modal sensor with an acceptable level of cross-modulation noise and compact architecture remains urgent.

7. Hybrid holographic WFS's

An individual line of research in the field of WFS's is the development of hybrid holographic sensors, in which WFS's of several types are integrated due to the use of one multiplexed hologram [47, 48]. For example, one can combine a zonal Shack–Hartmann sensor and a modal holographic sensor [47]. In this case, in contrast to the classical Shack–Hartmann sensor, a hologram in the form of an array of phase diffraction gratings with different periods and line orientations (rather than a lens array) is used to obtain a Hartmann pattern on the photodetector (Fig. 12a). After passing through this hologram and the lens installed behind it, wavefront portions are focused on the sensitive photodetector platform at the sites specified by diffraction grating parameters (Fig. 12b). This hologram is multiplexed with the hologram filtering aberration Zernike modes. As a result, when a wave passes through a multiplexed hologram, two spatially separated diffraction patterns are observed on the photodetector (Fig. 13), one of which (Hartmann pattern) is located at the centre and the other (determined by aberration Zernike modes) is on the periphery. In this hybrid WFS, the lower order aberrations are calculated according to the Hartmann pattern, and the higher order ones are determined from the difference in the intensities of pairs of symmetric spots on the periphery of photodetector sensitive platform. As was mentioned above, the measurement range of a modal holographic sensor is limited and depends on the amplitude of the aberration modes recorded in the filter hologram: the larger the amplitude of recorded aberrations, the wider the measurement range of the sensor and the lower its sensitivity are, and vice versa. Thus, the determination of lower order aberrations (which generally have the largest amplitude) from the Hartmann pattern allows one to extend the measurement range of modal holographic sensor without deteriorating its sensitivity.

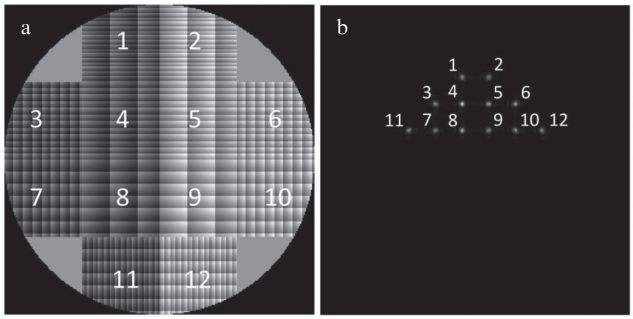

Figure 12. (a) Arrangement of phase diffraction gratings 1–12 on a hologram and (b) the Hartmann pattern obtained using this hologram. Reprinted with permission from [47] © The Optical Society.

In a similar way, having combined a modal holographic sensor with a curvature sensor, one can obtain a hybrid holographic WFS of another type [48]. In this case, the subhologram forming a Hartmann pattern on the photodetector sensitive platform is replaced with a subhologram composed of a

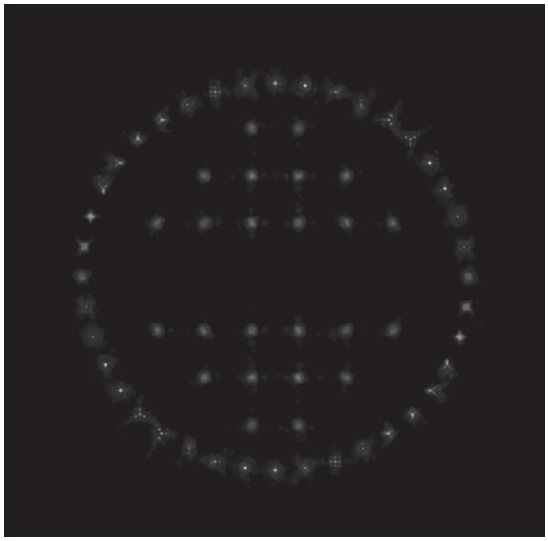

Figure 13. Two spatially separated diffraction patterns recorded by a hybrid holographic sensor. Reprinted with permission from [47] © The Optical Society.

hologram matrix of defocusing Z_4. Due to this hologram matrix, several pairs of spots are formed on photodetector, which correspond to local wavefront defocusings. The local wavefront defocusing value Z_4 on the corresponding portions is estimated from the difference in the intensities in each pair of spots. The local wavefront curvature in the subapertures corresponding to holograms from the matrix is proportional to local defocusing values Z_4. Furthermore, amplitudes of lower order aberrations are determined in correspondence with the standard operation algorithms of curvature sensor. The aforementioned subhologram is multiplexed with the second hologram, which filters aberration (nonlocal) Zernike modes. When this hybrid sensor operates as a component of adaptive system, dominant aberration modes are first measured using a curvature sensor and compensated for, after which the system is switched to a modal sensor. This approach allows one to reduce the number of correction cycles and, in the case of slow wavefront corrector, increase the operating speed of the system in comparison with an adaptive system based on a conventional holographic WFS [48].

8. Conclusions

In the nearest future the development of holographic WFS's will imply different ways of optimising their design in order to solve specific applied problems. It should be noted that the transition from recording filter holograms in photosensitive media (plates, films, etc.) to computer (digital) synthesis of holograms with their subsequent fabrication or reproduction on a spatial light modulator, which began in this century, will be continued. This approach is expected to reduce the errors caused by recording, yield a larger freedom in optimising a filter hologram, and simplify them. The studies aimed at increasing the number of aberration modes recorded by modal holographic WFS's will also be continued.

The development of holography as a whole and holographic WFS's in particular is directly related to the progress in the field of recording and synthesising holograms. In particular, the improvement of spatial phase modulators (increase in the frame rate to several tens of kHz or more, decrease in the pixel size, etc.) should give a strong impetus to the design of holographic WFS's, especially sensors with temporal multiplexing. The characteristics of holographic WFS's can also be significantly improved due to the development of new types of hologram carriers (holographic media), for example, those operating on the principles of plasmonics [49, 50].

Even now holographic WFS's make it possible to implement optical adaptive systems with a zonal corrector without any computer engineering. In future one will be able to design other types of optical adaptive systems on their basis, characterised by smaller sizes and lower cost and enhanced operating speed (up to several MHz or more).

References

1. Masters B.R. *Opt. Express*, **3** (9), 332 (1998).
2. Gourlay J., Love G.D., Birch P.M., Sharples R.M., Purvis A. *Opt. Commun.*, **137** (1–3), 17 (1997).
3. Salmon J.T., Bliss E.S., Long T.W., Orham E.L., Presta R.W., Swift C.D., Ward R.L. *Proc. SPIE*, **1542**, 2 (1991).
4. Liang J., Grimm B., Goelz S., Bille J.F. *J. Opt. Soc. Am. A*, **11** (7), 1949 (1994).
5. Li T., Huang L., Gong M. *Opt. Eng.*, **53** (4), 044101 (2014).
6. Puche A.B.P., Salerno L.C., Versaci F., Romero D., Alio J.L. *Eur. J. Ophthalmol.*, **29** (6), 585 (2019).
7. Agapito G., Pinna E. *J. Astronom. Telescop., Instrum. Syst.*, **5** (4), 049001 (2019).
8. Platt B.C., Shack R. *J. Refract. Surg.*, **17** (5), S573 (2001).
9. Brooks A.F., Kelly T.-L., Veitch P.J., Munch J. *Opt. Express*, **15** (16), 10370 (2007).
10. Baker K.L. *Opt. Express*, **14** (23), 10970 (2006).
11. Booth M.J., Neil M.A., Wilson T. *J. Opt. Soc. Am. A*, **19** (10), 2112 (2002).
12. Roider C., Jesacher A., Bernet S., Ritsch-Marte M. *Opt. Express*, **22** (4), 4029 (2014).
13. Loosen F., Stehr J., Alber L., Harder I., Lindlein N. *IEEE Photon. J.*, **10** (1), 1 (2018).
14. Feng F., White I.H., Wilkinson T.D. *J. Lightwave Technol.*, **32** (6), 1239 (2014).
15. Corbett A.D., Wilkinson T.D., Zhong J.J., Diaz-Santana L. *J. Opt. Soc. Am. A*, **24** (5), 1266 (2007).
16. Yao K., Wang J., Liu X., Lin X., Chen L. *Appl. Opt.*, **56** (23), 6639 (2017).
17. Jesacher A., Marshall G.D., Wilson T., Booth M.J. *Opt. Express*, **18** (2), 656 (2010).
18. Neil M.A.A, Booth M.J., Wilson T. *Opt. Soc. Am. A*, **17** (6) 1098 (2000).
19. Tyson R.K. *Principles of Adaptive Optics* (London: Academic Press Inc., 1991).
20. Kendrick R.L., Acton D.S., Duncan A.L. *Appl. Opt.*, **33** (27), 6533 (1994).
21. Lukin V.P. *Opt. Atmos.*, **2** (6), 563 (1989).
22. Antoshkin L.V., Botygina N.N., Emaleev O.N., Lukin V.P., Potanin S.F. *Opt. Atmos.*, **2** (6), 621 (1989).
23. Neil M.A.A., Booth M.J., Wilson T. *Opt. Lett.*, **25** (15), 1083 (2000).
24. Konwar S., Boruah B.R. *OSA Continuum*, **1** (1), 78 (2018).
25. Dong S., Haist T., Osten W., Ruppel T., Sawodny O. *Appl. Opt.*, **51** (9), 1318 (2012).
26. Kong F., Lambert A. *Appl. Opt.*, **55** (13), 3615 (2016).
27. Gavril'eva K., Gorelaya A., Fedorov E., Matital R.P., Orlov V., Shubenkova E., Venediktov V. *Proc. SPIE*, **10680**, 106802O (2018).
28. Anzuola E., Zepp A., Marin P., Gladysz S., Stein K., in *Imaging and Applied Optics* (OSA Techn. Digest, 2016) AOM4C.2.
29. Wilby M.J., Keller C.U., Snik F., Korkiakoski V., Pietrow A.G.M. *A&A*, **597**, A112 (2017).
30. Liu C., Xi F., Ma H., Huang S., Jiang Z. *Appl. Opt.*, **49** (27), 5117 (2010).
31. Mishra S.K., Bhatt R., Mohan D., Gupta A.K., Sharma A. *Appl. Opt.*, **48** (33), 6458 (2009).

32. Liu C., Xi F., Huang S., Jiang Z. *Appl. Opt*., **50** (11), 1631 (2011).
33. Liu C., Yang Y., Guo S., Xu R., Men T., Wen C. *Opt. Lasers Eng*., **51**, 1265 (2013).
34. Ghebremichael F., Andersen G.P., Gurley K.S. *Appl. Opt*., **47** (4), A62 (2008).
35. Palomo P.M., Zepp A., Gładysz S. *Proc. SPIE*, **9242**, 92421T (2014).
36. Bhatt R., Mishra S.K., Mohan D., Gupta A.K. *Opt. Lasers Eng*., **46**, 428 (2008).
37. Lacerenza M., Vera E., in *Latin America Optics and Photonics Conference* (OSA Techn. Digest, 2018) Tu4A.19.
38. Leyva D.G., Robertson B., Wilkinson T.D., Henderson C.J. *Appl. Opt*., **45** (16), 3782 (2006).
39. Yao K., Wang J., Liu X., Liu W. *Opt. Express*, **22** (14), 17216 (2014).
40. Kovalev M.S., Krasin G.K., Odinokov S.B., Solomashenko A.B., Zlokazov E.Yu. *Opt. Express*, **27** (2), 1563 (2019).
41. Ruchka P.A., Verenikina N.M., Gritsenko I.V., Zlokazov E.Yu., Kovalev M.S., Krasin G.K., Odinokov S.B., Stsepuro N.G. *Opt. Spectrosc*., **127** (4), 618 (2019).
42. Krasin G., Kovalev M., Odinokov S., Stsepuro N., Glukhov Yu. *Proc. SPIE*, **11056**, 1105629 (2019).
43. Orlov V.V. *Quantum Electron.*, **47** (8), 773 (2017) [*Kvantovaya Elektron*., **47** (8), 773 (2017)].
44. Orlov V.V., Venediktov V.Yu., Gorelaya A.V., Shubenkova E.V., Zhamalatdinov D.Z. *Opt. Laser Technol*., **116**, 214 (2019).
45. Andersen G., Ghebremichael F., Austin P.G., MacDonald K., Gaddipati R., Gaddipati P., in *Proc. Third AO4ELT Conf*. (Firenze, Italy, 2013).
46. Andersen G., Austin P.G., Gaddipati R., Gaddipati P., Ghebremichael F. *Opt. Express*, **22** (8), 9432 (2014).
47. Dong S., Haist T., Osten W. *Appl. Opt*., **51** (25), 6268 (2012).
48. Dong S., Haist T., Dietrich T., Osten W. *Proc. SPIE*, **9227**, 922702 (2014).
49. Genevet P., Lin J., Kats M.A., Capasso F. *Nature Commun*., **3**, 1278 (2012).
50. Cheng F., Ding L., Qiu L., Nikolov D., Bauer A., Rolland J.P., Vamivakas A.N. *Opt. Express*, **26** (23), 30678 (2018).